THE ASTRONOMICAL JOURNAL VOLUME 81, NUMBER 6 JUNE 1976

Diffraction calculation of occultation light curves in the presence of an isothermal atmosphere

Richard G. French and Peter J. Gierasch

Center for Radiophysics and Space Research, Cornell University, Ithaca, New York 14853

(Received 5 February 1976; revised 15 March 1976)

From diffraction theory, we calculate light curves for stellar occultations by a planetary body with an isothermal atmosphere. The character of the resulting curves is determined by the scale height H, the Fresnel zone size l, the surface atmospheric refractivity, and the planetary radius. We present an exact general solution and two approximations which are valid when $H \gg l$. Finally, we assess the importance of accounting for diffraction effects of the limb when deducing atmospheric parameters from occultation light curves.

INTRODUCTION

OBSERVATIONS of stellar and spacecraft occultations have been used to study the atmospheres of many solar system objects. For dense atmospheres, geometric optics has been used extensively (Baum and Code 1953; de Vaucouleurs and Menzel 1960; Brinkmann 1971; Hubbard *et al.* 1972; Veverka *et al.* 1974), while diffraction theory has been applied only in the case of a very thin atmosphere (Fjeldbo and Eschleman 1965) and the case of a perfectly conducting planetary surface (Adrianov 1969). In this paper we calculate occultation light curves from diffraction theory for an isothermal atmosphere of arbitrary surface density. In the next section we state the equations and assumptions used. We outline the exact solution and present approximations which are valid when the atmospheric scale height greatly exceeds the Fresnel zone scale. Sample results are given. In the final section we assess the validity of our assumptions. We conclude by considering the conditions under which limb diffraction must be taken into account when interpreting occultation light curves.

I. EQUATIONS AND ASSUMPTIONS

The occultation geometry is shown in Fig. 1. We model the planetary limb as a straightedge and the atmosphere as a phase screen. The theoretical occultation light curve is the diffraction pattern produced by this geometry. We assume a radially symmetric atmosphere with constant scale height much less than the planetary radius. The effects of surface roughness and conductivity are ignored. Finally, we assume a monochromatic point source at infinity. We discuss in Sec. II the extension of our results to more realistic conditions. Symbols are defined as follows:

λ = wavelength of observation,
D = distance to occulting body,
l $[= (\lambda D/2)^{\frac{1}{2}}]$ = Fresnel zone scale,
H = scale height,
R = radius of occulting body,
ϕ_0 = phase excess of grazing ray in radians,
ν_0 = refractivity of the atmosphere at the surface,
b $[= \phi_0 l^2/\pi H^2]$ = differential bending parameter,
y = distance along light curve from shadow boundary in units of l,
y_0 = location along light curve of line passing through occulted object and planetary limb.

Letting the preoccultation intensity be unity, we can express the intensity I at any point y along the light curve as (Sommerfeld 1964)

$$I = KK^*/2,$$

where

$$K = \int_{y_0}^{\infty} e^{i\theta(w)}dw, \qquad (1)$$

$$\theta(w) = \frac{\pi}{2}(w-y)^2 + \Phi(w),$$

where $\Phi(w)$ is the phase shift caused by the atmosphere. In general, ν_0 will depend upon λ, but we will ignore the effects of dispersion in this analysis. For an isothermal atmosphere, we find

$$\Phi(w) = \phi_0 \exp[-l(w-y_0)/H], \qquad (2)$$

where

$$\phi_0 = (2\pi)^{\frac{3}{2}}\frac{(RH)^{\frac{1}{2}}}{\lambda}\nu_0.$$

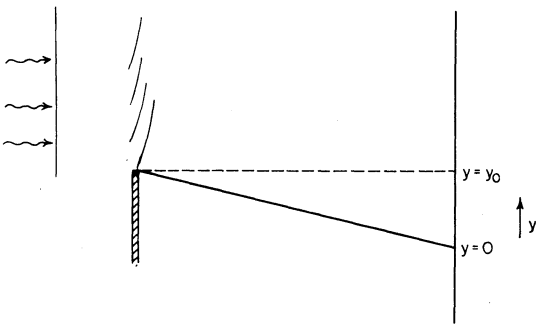

FIG. 1. Occultation geometry. A plane wave incident from an occulted object to the left intercepts a knife-edge and a phase screen, which model the surface of the planet and its atmosphere. The line at right represents the path of the Earth. The origin on the y axis is chosen so that the stationary phase point corresponding to $y = 0$ is at the knife-edge. This defines the position of the geometric shadow boundary. y is measured in units of l, the Fresnel zone scale.

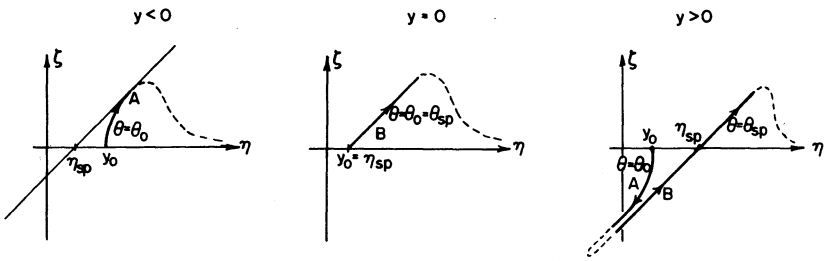

FIG. 2. The complex w plane. The integral is evaluated from $w=(y_0,0)$ to $w=(+\infty,0)$. Stationary phase paths are shown solid and integration paths are shown dashed for the cases $y<0$, $y=0$, and $y>0$. See text for explanation of symbols.

K is most easily evaluated by integrating along lines of stationary phase (i.e., constant θ) in the complex w plane. In this way, the rapidly oscillating integrand becomes a rapidly decaying exponential function. The geometry shown in Fig. 1 has the origin on the y axis chosen so that the stationary phase point corresponding to $y=0$ is at the knife-edge. This condition is met when $d\theta/dw=0$, whence

$$\pi(w-y)=(\phi_0 l/H)\exp[-l(w-y_0)/H]. \tag{3}$$

Evaluated at the knife-edge, where $y=0$ and $w=y_0$, this gives $y_0=\phi_0 l/\pi H$.

Letting $w=\eta+\iota\zeta$, we find

$$\begin{aligned}\mathrm{Re}\,(\theta)&=\frac{\pi}{2}[(\eta-y)^2-\zeta^2]\\&\quad+(\pi y_0 H/l)\exp[-l(\eta-y_0)/H]\cos(\zeta l/H),\end{aligned} \tag{4}$$

$$\begin{aligned}\mathrm{Im}\,(\theta)&=\iota\pi\{(\eta-y)\zeta\\&\quad-(y_0H/l)\exp[-l(\eta-y_0)/H]\sin(\zeta l/H)\}.\end{aligned}$$

Figure 2 illustrates schematically the paths of integration. The integrals along stationary phase paths A and B have respective phases, θ_0 and θ_{sp}:

$$\begin{aligned}&\text{along A:}\quad \theta_0=\frac{\pi}{2}(y_0-y)^2+\pi y_0 H/l;\\&\text{along B:}\quad \theta_{sp}=\frac{\pi}{2}(\eta_{sp}-y)^2+\pi H(\eta_{sp}-y)/l.\end{aligned} \tag{5}$$

The saddle point is located on the real axis at $w=\eta_{sp}$, and is defined by the solution to the equation

$$\eta_{sp}-y=y_0\exp[-l(\eta_{sp}-y_0)/H]. \tag{6}$$

The exact solution for the intensity requires numerical integration along the lines of stationary phase. The character of the resulting light curve depends upon the specified values of l, H, and ϕ_0. The diffraction fringe spacing is of order l, and the length scale of flux change from differential refractive bending is of order H. Differential refractive bending is important when the parameter $b=\phi_0 l^2/\pi H^2$ is of order unity or greater.

We have obtained solutions for a suite of values of l, H, and ϕ_0. Figure 3 presents two series of light curves for the cases $H=l$ and $H=10l$. The parameter b is varied to show the transformation of the light curve from a vacuum diffraction pattern to the geometric optics limit.

We have found two approximations to the exact solution which are valid under restricted circumstances. The first approximation utilizes the fact that the integral K in Eq. (1) can be expressed as a function of the usual Fresnel integrals as long as $\Phi(w)$ can be accurately represented by a second-order expansion in w over the significant range of contribution to the integral. The result is

$$I\approx\frac{1}{2(1+b)}\{[C(z)-\tfrac{1}{2}]^2+[S(z)-\tfrac{1}{2}]^2\}, \tag{7}$$

where

$$z=\frac{\pi y^2}{2(1+b)},$$

$$\begin{matrix}C(z)\\S(z)\end{matrix}=\int_0^z\begin{matrix}\cos\\\sin\end{matrix}\frac{\pi}{2}t^2dt.$$

The condition for validity of the approximation is

$$\begin{aligned}&\phi_0[l(w-y_0)/H]^3/b\ll\pi/2\\&\text{or, equivalently,}\\&b[l(w-y_0)]^3/3H\ll 1.\end{aligned} \tag{8}$$

in the range of w for which there is significant contribution to the integral K in Eq. (1). This range cannot be defined precisely, but is certainly several tens of Fresnel zones from y. In practice, this restricts the application of Eq. (7) to instances where $H/l\gg 1$ and $b\ll 1$. The approximation is increasingly accurate as the shadow boundary is approached (i.e., as $y\to 0$). These results are in agreement with those of Fjeldbo and Eschleman (1965), but we emphasize that the requirement of a low-density atmosphere is not sufficient; in addition, the Fresnel zone scale must be much less than the scale height. For a distant object such as Pluto, this last condition may not be satisfied.

We have obtained another approximation which is valid for an arbitrarily dense atmosphere and reproduces the entire light curve away from the shadow boundary as long as $H\gg l$. In this case, we approximate the stationary phase paths A and B in Fig. 2 as straight lines over the region of major contribution to the integral. The complex integrations can then be performed analytically. The results follow.

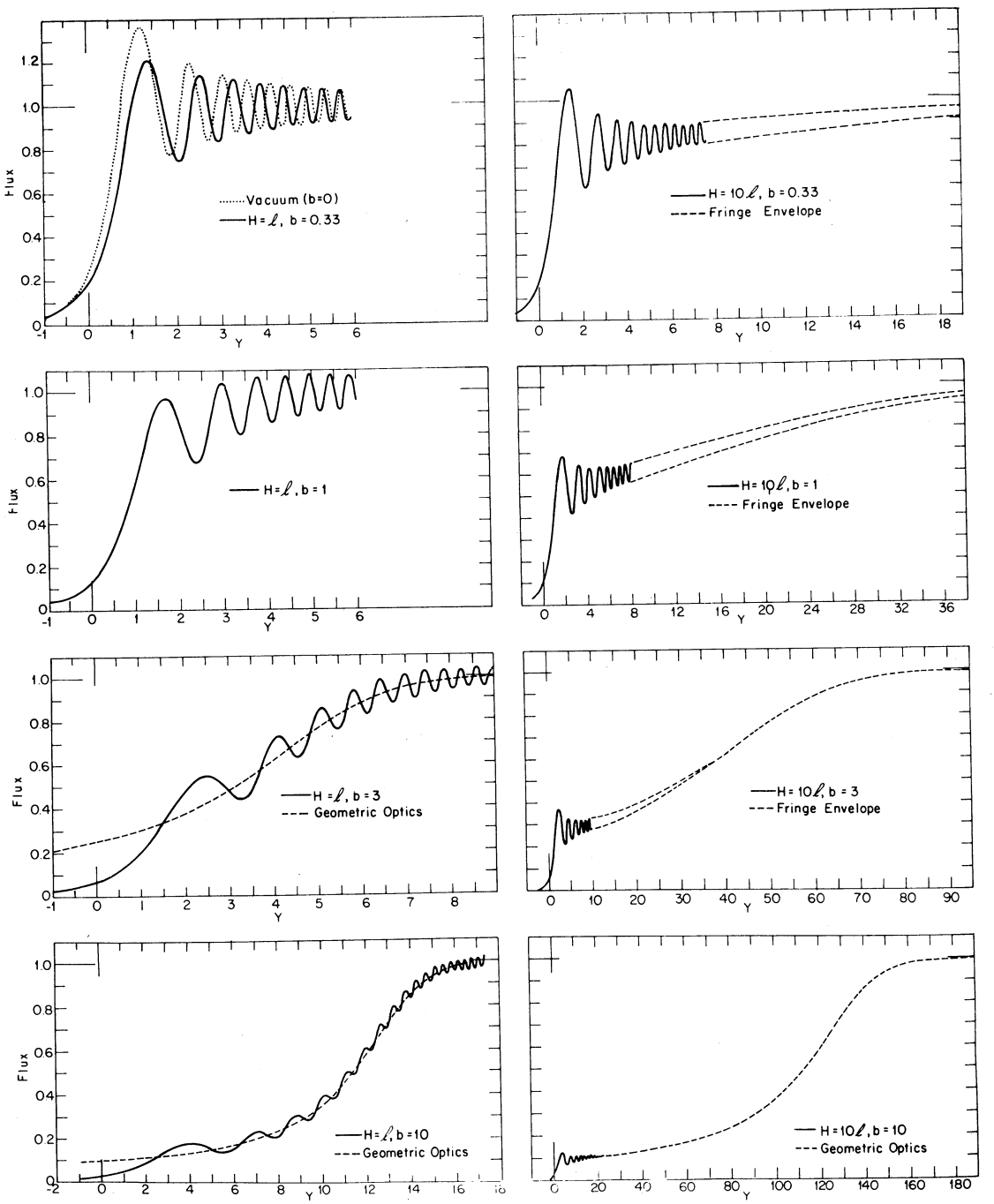

FIG. 3. Model light curves for occultations of a monochromatic point source. The effect of increasing the amount of atmosphere (equivalent to increasing parameter b) is shown from top to bottom as the transition from a vacuum diffraction pattern to the geometrical optics result of Baum and Code (1953). Curves on the left have $H/l=10$; on the right, $H/l=1$. Note the changes in scale along the y axis.

As in the exact solution, $I=KK^*/2$. For the entire bright region away from the shadow boundary ($y>0$),

$$I\approx\left|\frac{K_B}{2}\right|^2\left[1+\left|\frac{K_A}{K_B}\right|^2+2\left|\frac{K_A}{K_B}\right|\cos(\theta_0-\theta_{sp}-3\pi/4)\right], \quad (9)$$

where

$$\begin{aligned}\theta_0-\theta_{sp}&\approx\pi y^2\{1-[b/(1+b)]^2\}/2,\\ |K_A|&=1/\pi y,\\ |K_B|&=\{2/[1+l(\eta_{sp}-y)/H]\}^{\frac{1}{2}}.\end{aligned} \quad (10)$$

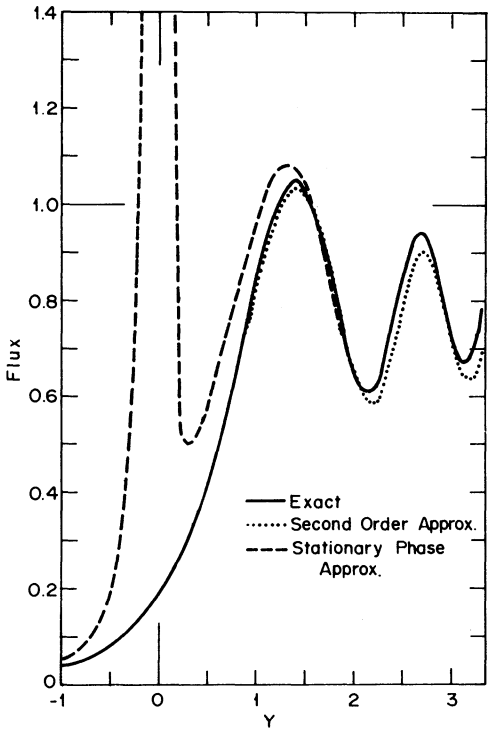

FIG. 4. Comparison of exact and approximate solutions. The exact curve has parameters $H/l=10$, $b=0.33$. Notice that a small segment of the true solution is not matched by either approximation. For larger H/l and smaller b this segment disappears, while for smaller H/l and larger b the approximations are less and less accurate.

Far from the shadow boundary, the transcendental equation (6) must be solved for η_{sp}. For the first few fringes, we may use the approximation

$$\eta_{sp}-y_0\approx y/(1+b),$$

and Eq. (10) can be rewritten as

$$|K_B|\approx\left\{2\Big/\left[1+b\left(1-\frac{yl}{H(1+b)}\right)\right]\right\}^{\frac{1}{2}}$$

$$\text{for } y-y_0\approx 0(1). \quad (11)$$

It can be shown that this stationary phase expansion is equivalent to the analogous geometric optics result whenever $|K_A/K_B|\ll 1$. In this case, $I\approx|K_B|^2/2$. From Eqs. (6) and (10), this can be recast in the form

$$y=y'-\frac{H}{l}\left[\left(\frac{1}{I}-2\right)+\ln\left(\frac{1}{I}-1\right)\right], \quad (12)$$

where

$$y'=H[b+\ln(b)-1]/l.$$

This is just the Baum and Code equation for an occultation light curve assuming geometric optics and constant scale height (Baum and Code 1953).

For the dark region, $y<0$, away from the shadow boundary,

$$KK^*\approx|K_A|^2=(1/\pi y)^2. \quad (13)$$

Because of the singularity of K_A at $y=0$, the approximation breaks down near the shadow boundary, for $|y|\lesssim 2$. Equation (7) provides a better approximation to the light curve in this region.

By combining these two approximations, accurate light curves can easily be generated when $b\ll 1$, $H/l\gg 1$. Near the shadow boundary, the intensity is accurately given by Eq. (7), and far from the shadow boundary, the intensity is given by Eq. (9). As b is increased, Eq. (7) is less and less accurate. Eventually, there will be a segment of the light curve which is not accurately reproduced by either approximation. Figure 4 shows a comparison of exact and approximate solutions at a value of b for which the expansion approximation is beginning to break down. In this case, the second-order expansion is accurate only for y less than about 2, while the stationary phase approximation holds for y greater than about 1.5. Notice that the approximate stationary phase method is valid for arbitrary b; that is, for an arbitrarily dense atmosphere. As b becomes of order unity, the important length scale for the light curve is H, and the uncertain region near the shadow boundary becomes less significant since it corresponds to only a few Fresnel zones. If required, the exact solution for this segment can be obtained numerically by integrating Eq. (1) along stationary phase paths defined by Eq. (5).

II. DISCUSSION

A. Limitations of the Theory

In the preceding calculations, we have ignored several complications which make occultation observations difficult to interpret. Our assumption that the atmosphere is radially symmetric and of constant scale height is simplistic, but is a reasonable starting point and, as in the case of geometric optics, renders the problem analytically tractable. Consideration of diffraction effects of atmospheric inhomogeneities, turbulence, scintillation, and other complexities will ultimately be important but seems premature at this stage. Andrianov (1969) shows that a perfectly conducting spherical surface can modify occultation light curves, but at optical wavelengths perfect conductivity is a poor approximation and we feel safe in ignoring such effects. Calculations by Evans (1970) indicate that planetary surface irregularities can cause distortion of vacuum diffraction patterns when the irregularities are of order l in size. This is significant for lunar occultations when l is only a few meters, but for planetary observations with l several hundred meters or more, the problem is much less severe.

The combined tendency of finite optical bandpass and finite star size to smooth out features in the light

TABLE I. Surface atmospheric refractivity ν_0 and number density n_0 for $b=1$. See text for discussion of choice of H and other details.

Occulting object	D(AU)	l(km) ($\lambda=4400$ Å)	H(km)	H/l	ν_0	n_0(cm^{-3})
Io	4.2	0.37	15	40.3	8.7×10^{-10}	7.8×10^{13}
Ganymede	4.2	0.37	15	40.3	7.2×10^{-10}	6.5×10^{13}
Rhea	8.5	0.53	15	28.3	7.1×10^{-10}	6.4×10^{13}
Titania	18.2	0.77	15	19.4	3.8×10^{-10}	3.4×10^{13}
Triton	29.1	0.98	15	15.2	1.2×10^{-10}	1.1×10^{13}
Pluto	31.0	1.01	1	0.9	1.5×10^{-12}	1.4×10^{11}
			5	4.4	1.7×10^{-11}	1.5×10^{12}
			15	13.3	8.8×10^{-11}	7.9×10^{12}
			25	22.2	1.9×10^{-10}	1.7×10^{13}

curve is important and has been discussed extensively in the literature (see, e.g., Nather and McCants 1970). Elliot *et al.* (1975) consider in detail the problem of convolving a stellar image with the light curve.

B. Application of the Theory

Under what circumstances must we account for limb diffraction effects in the proper interpretation of occultation light curves? The atmosphere must be thin enough for diffraction effects of the planetary limb to be important. In our parlance, "thin enough" means that the parameter b must not greatly exceed unity, as can be seen in Fig. 3. From the definition of b, this condition can be stated as

$$b=(2\pi R/H)^{\frac{1}{2}}\nu_0 D/H \lesssim 1. \qquad (14)$$

When $b\gg1$, as in the case of most occultations by planets, limb diffraction is unimportant. This is the case, for example, in the 1976 occultation of ϵ Geminorum by Mars and the 1977 occultation of SAO 158687 by Uranus. Table I lists the surface atmospheric refractivity ν_0 and number density n_0 of several planetary objects for the case $b=1$, when diffraction effects and differential refractive bending are both important. Number densities are calculated for an atmosphere whose refractivity is 3×10^{-4} at STP; this value is appropriate for N_2 (Allen 1973). Also shown are the Fresnel zone scale for $\lambda=4400$ Å and the scale height. The scale height is difficult to estimate, and is in fact one of the unknowns which occultation data could permit us to determine. For Pluto, we know none of the parameters which define the scale height of the putative atmosphere, and a range of guesses for H is given. For the other objects, we take $H=15$ km as reasonable for an atmosphere of N_2, but we attach no deep significance to this choice. The nature of the resultant occultation curves can be seen in each case by comparison of Fig. 3 for the appropriate values of b and H/l.

It is not enough to know when limb diffraction is theoretically important. We must also determine the observational conditions under which we could perceive its effects in an occultation curve. Fringes, the characteristic signature of limb diffraction, will be badly smeared whenever the stellar image is much greater than l at the occulting object. Thus, a star with too large an angular diameter will mask all fringes. Additionally, there must be enough light from the star to resolve fringes in the noise. We have attempted to quantify the requirements for limb diffraction to be visible in a light curve, assuming that the atmosphere is thin in the sense defined above. We do not consider the case of occultations using spacecraft, which requires special consideration. For the size of the stellar image at the occulting body to be less than h, the apparent magnitude of the occulted star must be at least as large as $m_{\min}$:

$$m_{\min}=M-5+5\log_{10}(2R_\odot D/h), \qquad (15)$$

where M is the absolute stellar magnitude, $R_\odot$ is the stellar radius, and D is the distance to the occulting body; the argument of the logarithm is in parsecs. When h is of order l, only the first few fringes survive the convolution process, as can be seen in Fig. 5.

A star must be far enough away to avoid washing out the diffraction pattern, but if it is too far away, there

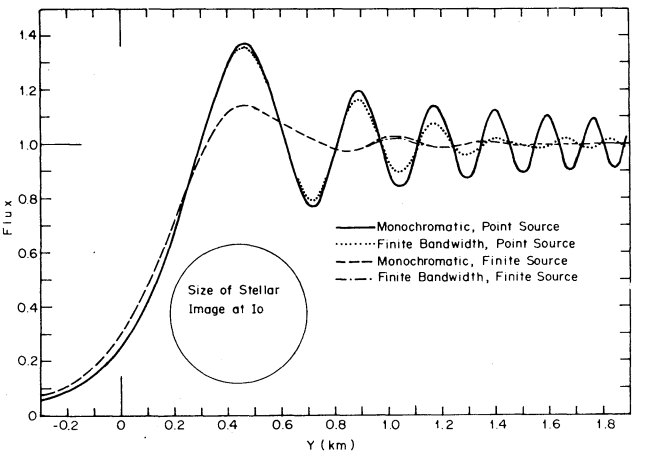

FIG. 5. Effects of finite bandpass and stellar image on occultation light waves. Parameters used to generate these curves are appropriate for the occultation of β Sco C by Io (Bartholdi and Owen 1972). Central wavelength of filter 4400 Å; filter bandwidth is 1000 Å; stellar image size at Io, given by h in Eq. (15), is $1.34l$. We assume $b=0$ and ignore stellar limb darkening.

TABLE II. Range of acceptable apparent magnitudes of main-sequence stars occulted by a number of objects. m_{max}, calculated for telescope apertures of 44 and 88 in., represents a minimum brightness which will allow detection of diffraction fringes. m_{min} represents an upper limit on the size of the stellar image at the occulting object. When m_{min} exceeds m_{max}, fringes cannot be detected. See text for the criteria which define a detection, and for the assumptions involved in calculating m_{max} and m_{min}.

Occulting object	D(AU)	m_{max}(44 in.)	m_{max}(88 in.)	m_{min} for given main sequence spectral class				
				O5	B5	A5	F5	G5
Io, Ganymede	4.2	7.9	9.4	4.9	6.2	7.6	8.2	9.4
Rhea, Titan	8.5	8.0	9.5	5.6	7.0	8.4	9.0	10.1
Titania	18.2	8.3	9.8	6.4	7.8	9.2	9.8	10.9
Triton	29.1	8.5	10.0	7.0	8.3	9.7	10.3	11.5
Pluto	31.0	8.5	10.0	7.0	8.4	9.8	10.4	11.5

will not be enough light to resolve fringes in the noise. We specify N_{min}, the minimum photon counting rate necessary to resolve fringes, by the following relation;

$$N_{min} = 2n_l v/l(\Delta I)^2. \quad (16)$$

Here, n_l is the number of points per Fresnel length l that we want to observe with an accuracy of ΔI, a given fraction of the unocculted intensity. The velocity of the stellar image perpendicular to the limb of the occulting body is given by v. The factor of 2 is present because we demand that the fringes be resolvable when the intensity is half its unocculted value. Equation (17) relates N_{min} to the maximum apparent magnitude m_{max} of the occulted star which will still permit detection of fringes.

$$m_{max} = m_{ref} - 2.5 \log_{10}(N_{min}/\epsilon A \Delta\lambda N_{ref}). \quad (17)$$

N_{ref} is the number of photons/cm^2 sec Å reaching the Earth from a star of apparent magnitude m_{ref}. A is the collecting area of the telescope in (centimeters)^2, $\Delta\lambda$ is the optical filter bandwidth in angstroms and, ϵ is a factor describing the efficiency of the filters, optics, and photomultipliers used in the observation. Assuming that the atmosphere is thin, the requirement for an occultation to exhibit the effects of limb diffraction is

$$m_{min} \leq m_{ap} \leq m_{max}. \quad (18)$$

Here, m_{ap} is the apparent magnitude of the occulted star.

We have calculated m_{max} and m_{min} for a range of possible occultations. The results are given in Table II. In calculating m_{min}, main-sequence stellar radii and absolute magnitudes were taken from Allen (1973), and we let $h = l$, for a central filter wavelength of 4400 Å. We determined m_{max} for telescope apertures of 44 and 88 in., and we used $n_l = 5$, $\Delta I = 0.02$, $\Delta\lambda = 800$ Å, and $\epsilon = 0.20$. N_{ref} was taken as 10^3 sec^{-1} cm^{-2} Å^{-1} for $m_{ref} = 0.00$. We used as a basis that the 5550 Å monochromatic flux reaching the Earth for $V = 0.0, B - V = 0.0$ is 3.58×10^{-9} erg sec^{-1} cm^{-2} Å^{-1} (Latham 1970).

Table II is intended to be suggestive, rather than prescriptive. Its results were calculated on the basis of primitive notions of what constitute acceptable data for fringe detection. The use of least-squares fitting techniques in analyzing the data would have the effect of raising m_{max}. On the other hand, noise introduced by light from the occulting body will tend to lower m_{max}. The problem of data analysis in the presence of noise is complex and in the case of occultation light curves remains to be addressed in detail. Occultation probabilities have been studied by a number of authors (see, e.g., O'Leary 1972) and we do not discuss them here. It is clear, however, that occultations of stars with magnitudes less than m_{max} are rare.

Of all past observations known to us (other than lunar events) only Bartholdi and Owen (1972), in the occultation of β Sco C by Io, present evidence for diffraction fringes. Even here, the identification cannot be regarded as certain. Figure 7 of their paper shows that the length scale of the fringes in their best fit is much shorter than the coherence interval of the noise in their data. Additionally, the maximum predicted fringe amplitude is 15% of the unocculted flux, while the data show intensity variations as large as 35% just prior to the onset of the occultation. (Notice that the abscissa in their Fig. 7 should be labeled in thousands, not hundreds, of meters.) The lack of correlation between ingress and egress curves is further cause for concern. In spite of these problems, their observations provide the best data that we have so far. However, stellar occultations by asteroids occur relatively frequently and careful observation may permit diffraction fringes to be observed. While not providing atmospheric information, analysis of fringe spacing could allow determination of asteroid diameters from a single observation (Elliot 1976). An excellent opportunity for observers in western North America to apply this technique will occur on 10 October 1976 (UT), when Pallas occults SAO 153844 (Taylor 1976).

Even given a light curve with definite fringes, it is not an easy task to deduce atmospheric characteristics. There are seven unknowns to be determined:

(1) the $I = 1$ flux level,
(2) The $I = 0$ flux level,
(3) v,
(4) the $y = 0$ point,
(5) the nature of the stellar image, both size and limb darkening characteristics,
(6) atmospheric scale height H,

(7) b; or, equivalently, the atmospheric refractivity at the planetary surface.

Additionally, the effects of finite bandwidth must be accounted for, although as seen in Fig. 5, the influence of finite star size is much more important for reasonable filter bandwidths. Even for $\Delta\lambda/\lambda$ as large as 0.23, the first two fringes differ only slightly from the monochromatic results. Since signal-to-noise constraints and finite star size limit attention to the first few fringes in any case, there seems to be little advantage in using narrow-bandwidth filters for this class of occultations. Nather and McCants (1970) discuss a number of model-fitting techniques which could be modified for data analysis in this application.

Theoretically, the slope of the light curve at $y=0$ can be used to determine b, but in practice uncertainties in v and convolution with the stellar image will make this difficult. Simultaneous observations at several locations would allow an accurate determination of v. By observing at several different wavelengths, the fringes can be checked, since fringe location is wavelength dependent, while the geometric optics light curve features, due to differential bending, depend only on H and v.

ACKNOWLEDGMENTS

This work was supported in part by NASA Grant NGL 33–010–186. One of us (P.J.G.) acknowledges the support of an Alfred P. Sloan research fellowship.

REFERENCES

Adrianov, V. A. (1969). "Effect of the atmosphere of a planet on Fresnel diffraction of ultrashort radiowaves," Radiotekh. Elektron. **14**, 1355.
Allen, C. W. (1973). *Astrophysical Quantities* (Athlone, London).
Bartholdi, P., and Owen, F. (1972). "The occultation of Beta Scorpii by Jupiter and Io. II. Io," Astron. J. **77**, 60.
Baum, W. A., and Code, A. D. (1953). "A photometric observation of the occultation of σ Arietis by Jupiter," Astron. J. **58**, 108.
Brinkmann, R. T. (1971). "Occultation by Jupiter," Nature **230**, 515.
Elliot, J. L. (1976). In preparation.
Elliot, J. L., Wasserman, L. H., Ververka, J., Sagan, C., and Liller, W. (1975). "Occultation of β Scorpii by Jupiter. V. The emersion of β Scorpii C," Astron. J. **75**, 323.
Evans, D. S. (1970). "Photoelectric measurement of lunar occultations. III. Lunar limb effects," Astron. J. **75**, 589.
Fjeldbo, G., and Eshleman, V. R. (1965). "The bi-static radar-occultation method for the study of planetary atmospheres," J. Geophys. Res. **70**, 3217.
Hubbard, W. B., Nather, R. E., Evans, D. S., Tull, R. G., Wells, D. C., van Citters, G. W., Warner, B., and VandenBout, P. (1972). "The occultation of Beta Scorpii by Jupiter and Io. I. Jupiter," Astron. J. **77**, 41.
Latham, D. W. (1970). "Abundances of the elements in Sirius and Merak," Smithsonian Astrophys. Obs. Special Rep. No. 321.
Nather, R. E., and McCants, M. M. (1970). "Photoelectric measurements of lunar occultations. IV. Data analysis," Astron. J. **75**, 963.
O'Leary, B. (1972). "Frequencies of occultations of stars by planets, satellites, and asteroids," Science **175**, 1108.
Sommerfeld, A. (1964). *Optics* (Academic, New York).
Taylor, G. (1976). Private communication.
deVaucouleurs, G., and Menzel, D. H. (1960). "Results of the occultation of Regulus by Venus, July 7, 1959," Nature **188**, 28.
Veverka, J., Wasserman, L. H., Elliot, J., Sagan, C., and Liller, W. (1974). "The occultation of β Scorpii by Jupiter. I. The structure of the Jovian upper atmosphere," Astron. J. **79**, 73.